# Small retinal vessels extraction towards proliferative diabetic retinopathy screening

Girish Singh Ramlugun [a], Vivek Krishna Nagarajan [a], Chandan Chakraborty [b],*

[a] Department of Biomedical Engineering, Manipal Institute of Technology, Manipal, Karnataka, India
[b] School of Medical Science & Technology, IIT Kharagpur, India

## ARTICLE INFO

*Keywords:*
Proliferative diabetic retinopathy
Gabor filter
Hysteresis thresholding
CLAHE

## ABSTRACT

This paper introduces a systematic approach for segmentation of retinal blood vessels towards the diagnosis of proliferative diabetic retinopathy (PDR) from digital fundus images. Here, 2D-Match (Gabor) filters are used on digital fundus images in which the vessels are enhanced by contrast-limited adaptive histogram equalization (CLAHE). A double sided thresholding scheme is then used to segment the vessels. Hysteresis thresholding is performed with the large and small vessels clipped at different intensity levels in order to reconstruct the vessels in the image. This vessel extraction technique leads to high accuracy (93.1%) in comparison with the ground truth images provided in the DRIVE database.

© 2011 Elsevier Ltd. All rights reserved.

## 1. Introduction

Vessel extraction is important in the analysis of digital fundus images since it helps in diagnosing retinal diseases, especially in assessing the severity of the disease in borderline cases. The medical motivation towards the segmentation of blood vessels of retinal images is to suppress the background and accentuate the small vessels so that features such as abnormal branching, tortuosity, entropy, neovascularization become more visually prominent. These clinical markers help ophthalmologists in diagnosing various retinopathies especially diabetic retinopathy (DR), which is a major complication of diabetes. According to the World Health Organization (WHO), more than 220 million people worldwide have diabetes, and deaths due to diabetes are expected to double between 2005 and 2030. Also, the WHO claims that screening for diabetic retinopathy is a cost saving intervention which will help in reducing the burden of diabetes (World Health Organization Media Centre, 2009).

The main problem faced in vessel extraction of low resolution images is the efficient extraction of the smaller vessels. This is because during conventional pre-processing techniques like smoothing and normal histogram equalization, the smaller vessels get averaged out with the background. This results in the fusing of these vessels with the background, making it difficult to segment them out because of the low contrast with the background. Hence small vessel enhancement algorithm is applied to the retinal images for better accurate results. Though the small vessels are

enhanced, the accuracy of the results would also depend on the efficiency of the vessel segmentation algorithm. It should be able to remove other structures like the optic disc, fovea centralis, etc. and extract only the retinal vessels, as false detections affect the accuracy of the result.

In the literatures, some attempts have already been made to extract retinal vessels from fundus images. Amongst these, scale-space analysis and region growing, mathematical morphology and curvature estimation, verification-based local thresholding, pixel classification, matched filter methods (Niemeijer, Staal, Van Ginneken, Loog, & Abràmoff, 2009), etc. are useful for vessel extraction in totality, but less attention has been given towards small vessel extraction. Matched filtering approaches such as Odstrčilík, Jan, Gazárek, and Kolář (2009) and Zhang, Li, You, and Zhang (2009) have been recently proposed. Zhang et al. (2009) emphasize on the detection of neovascularizations in case of proliferative diabetic retinopathy (PDR). In fact, the brightness level varies over different regions within the image viz., optic disc region is significantly brighter than rest. In such situation, global contrast enhancement technique is not a suitable preprocessing method. Furthermore, the brighter regions need to be suppressed so that the vessels of that region become more prominent. In the diagnostics of PDR, it is meaningful to consider the vessels in the optic disc region. In view of this, we here propose a computer-assisted methodology wherein contrast limited adaptive histogram equalization (CLAHE) is used to preprocess the retinal images.

The images and database used are described in Section 2.1. Section 2.2 deals with the framework of our segmentation method based on the 2D-Gabor filter and double-sided thresholding method. In Section 3, results are shown and discussed in order to show its novelty.

---

\* Corresponding author. Tel.: +91 3222 283570.
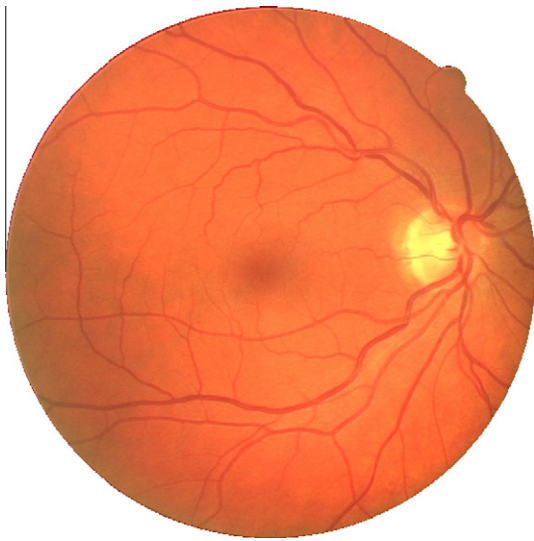E-mail address: chandanc@smst.iitkgp.ernet.in (C. Chakraborty).

**Fig. 1.** Original fundus retinal image.

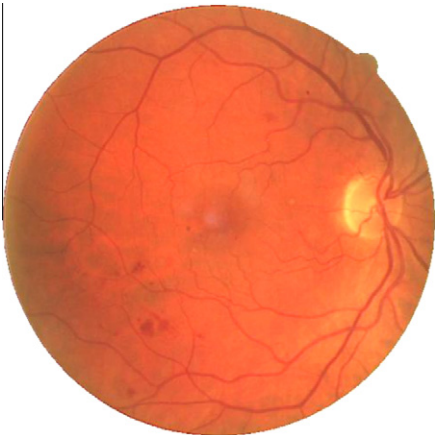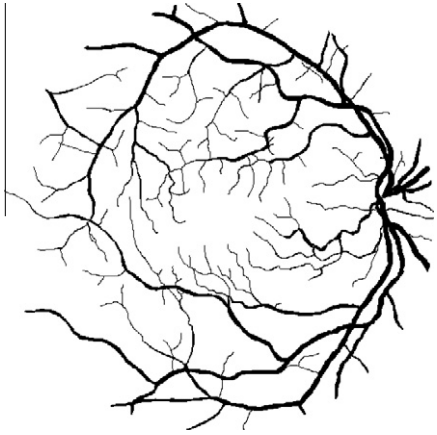## 2. Materials and methods

### 2.1. Retinal imaging and acquisition
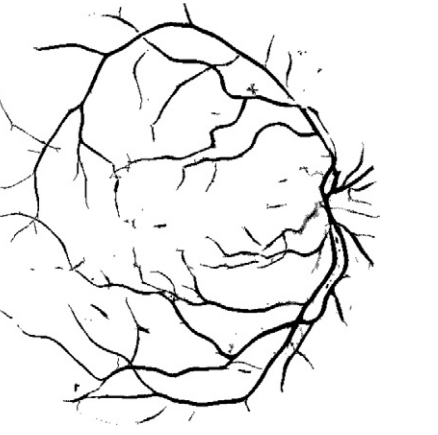
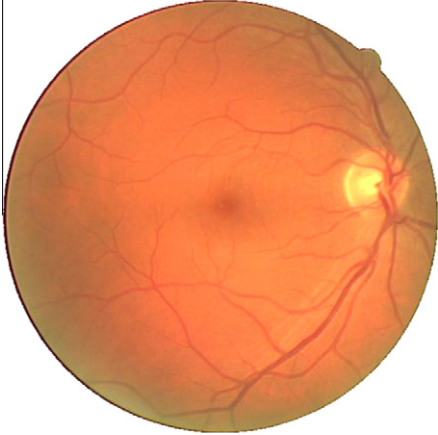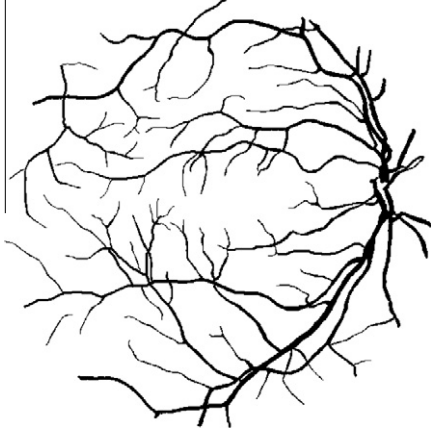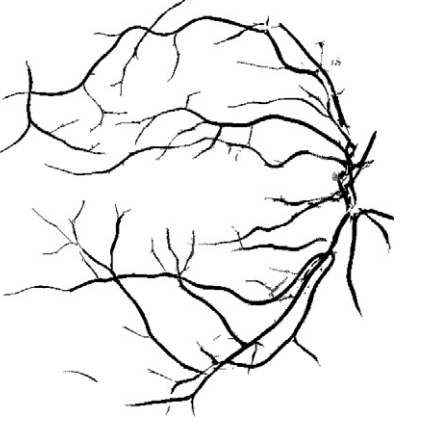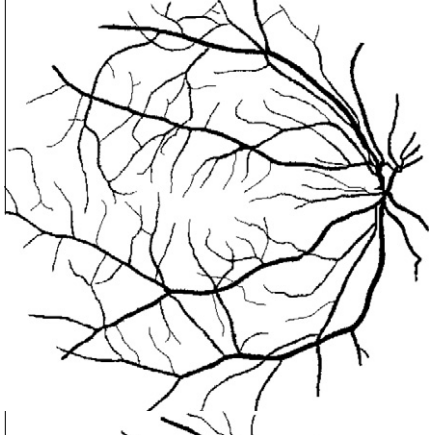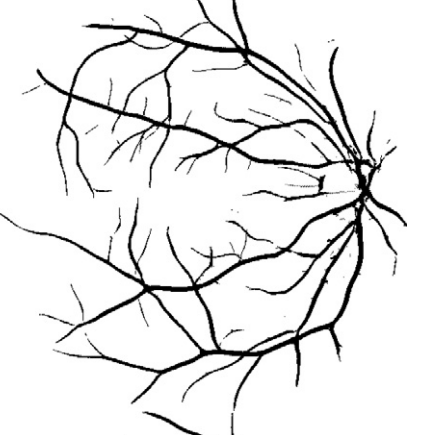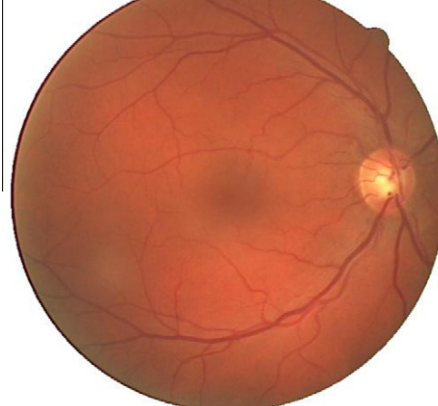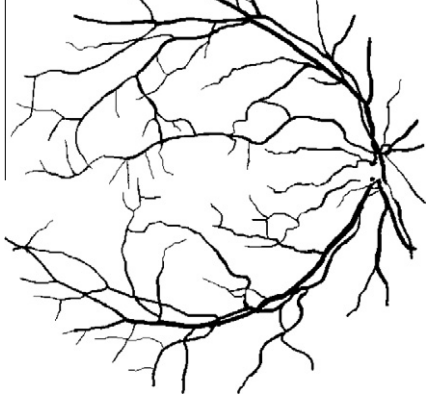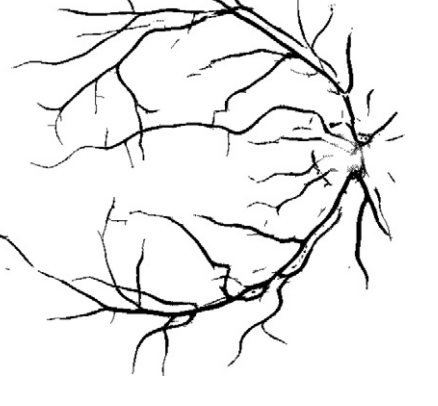In this study, the fundus images are downloaded from DRIVE database (http://www.isi.uu.nl/Research/Databases/DRIVE/). These retinal photographs were obtained from a diabetic retinopathy screening program in Netherlands. The screening population consisted of 400 diabetic subjects between 25 and 90 years of age. Forty photographs have been randomly selected, 33 do not show any sign of diabetic retinopathy and 7 show signs of mild early diabetic retinopathy. Each image has been JPEG compressed. The images were acquired using a Canon CR5 non-mydriatic 3CCD camera with a 45° field of view (FOV). Each image was captured using 8 bits per color plane at 768 × 584 pixels. The FOV of each image is circular with a diameter of approximately 540 pixels. For this database, the images have been cropped around the FOV. For each image, a mask image is provided that delineates the FOV. Fig. 1 shows a sample of the input image we have used in this paper.

**Table 1**
The segmentation results using the proposed scheme are provided along with its ground truths.

| Original image | Ground truth vessels | Reconstructed vessels by our scheme |
|---|---|---|

**Table 1** (*continued*)

| Original image | Ground truth vessels | Reconstructed vessels by our scheme |
| --- | --- | --- |

## 2.2. Methodology

The following flow diagram represents the framework of our segmentation method.

**Input Image**

Color Retinal Fundus Image

Green Channel image

| Apply CLAHE, with a low clip limit ($\beta$) | Apply CLAHE, with a high clip limit ($\beta$) | Apply CLAHE, with a low clip limit ($\beta$) |
|---|---|---|
| Obtain Gabor Kernels for small vessels by using $\sigma=1.3$ | Obtain Gabor Kernels for small vessels by using $\sigma=1.3$ | Obtain Gabor Kernels for large vessels by using $\sigma=5.8$ |
| Rotate kernel in 12 different directions with $15^0$ spacing | Rotate kernel in 12 different directions with $15^0$ spacing | Rotate kernel in 12 different directions with $15^0$ spacing |
| Convolve the kernels separately with the pre-processed image | Convolve the kernels separately with the pre-processed image | Convolve the kernels separately with the pre-processed image |
| Perform double sided thresholding in x and y direction | Perform double sided thresholding in x and y direction | Perform double sided thresholding in x and y direction |
| Scan the resultant of each image in x and y direction and choose max response | Scan the resultant of each image in x and y direction and choose max response | Scan the resultant of each image in x and y direction and choose max response |
| Form a vessel map ($V_{sh}$) by choosing max response from each thresholding result. | Form a vessel map ($V_{sl}$) by choosing max response from each thresholding result. | Form a vessel map ($V_{lh}$) by choosing max response from each thresholding result. Obtain $V_{ll}$ by thresholding at a lower value |

Reconstruction by performing hysteresis thresholding to form small Vessel Map ($V_s$) by using ($V_{sh}$) as marker and ($V_{sl}$) as mask

Reconstruction by performing hysteresis thresholding to form large Vessel Map ($V_l$) by using ($V_{lh}$) as marker and ($V_{ll}$) as mask

Fuse the two images to form the Final Vessel Map ($V_f$) from $V_s$ and $V_s$
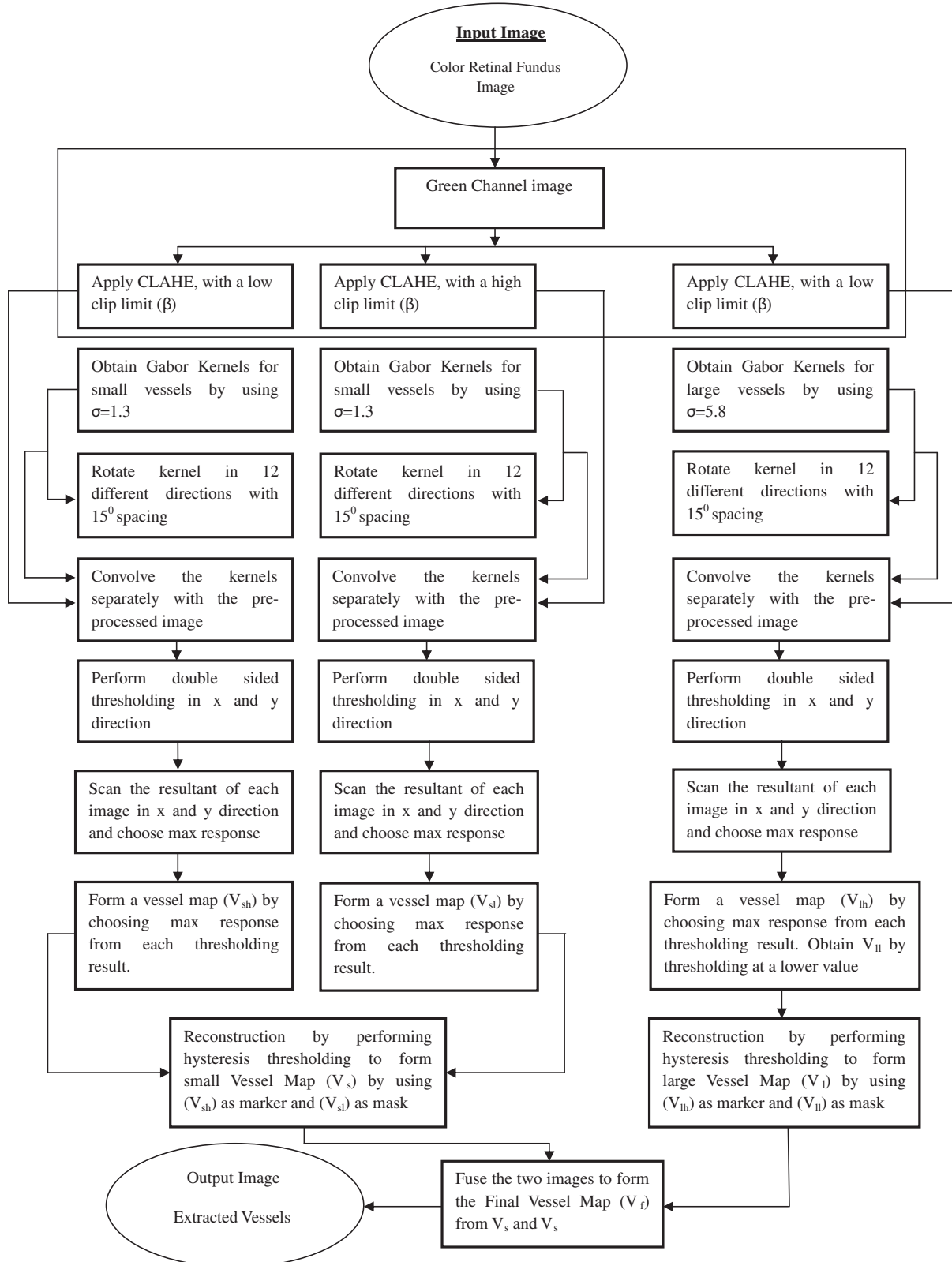
Output Image

Extracted Vessels

**Fig. 2.** Histogram equalized image of green channel of input.

### 2.2.1. Preprocessing

As we can see in the flow chart, this algorithm is specially designed to extract the smallest vessels from the input image. The green channel image contains the most amount of information since there is a higher contrast between the vessel pixels and the non-vessel pixels (Al-Rawi, Qutaishat, & Arrar, 2009).

Global based contrast enhancement techniques do not produce efficient results as the retinal image has different brightness regions such as the optic disk, macular region, etc. (Alex Stark, 2000; Pang et al., 2009). Hence CLAHE is used for enhancing the retinal vasculature adaptively. The image is divided into $8 \times 8$ tiles and histogram equalization is applied locally to each of the non overlapping contextual regions (Fig. 2). Clipping of the local histograms using a clip limit ($\beta$) ensures that the local contrast is limited and not increased to maximum.

Since the large vessels are easily differentiated from the background because of their inherent high contrast, we use a low clip limit for the CLAHE. For small vessels, we need to apply a higher clip limit because of their low contrast difference with the background. However, using a high clip limit also increases the noise in the image, thus increasing the probability of obtaining false detections. To counter this problem, we use a hysteresis thresholding algorithm proposed in Reza (2004).

### 2.2.2. Retinal vessel segmentation

After applying the different clip limits to the images, we use the 2D Gabor matched filter approach for segmentation. The matched filter approach was first proposed by Chaudhuri et al. (1989). The retinal vessel is a tube like structure whose cross section can be mathematically correlated to a Gabor response (Zhang, Wu, & Liu, 2005). We have used a truncated 2D Gabor response filter to create a set of 12 templates, each being defined at an interval of $15°$. This is to be able to cater for vessels with different orientations. The Gabor response filter is given by

$$G(x,y) = exp\left\{-\left(\frac{x_1^2}{\sigma_x^2} + \frac{y_1^2}{\sigma_y^2}\right)\right\} \cos\left(\frac{2\pi x_1}{\lambda}\right) \quad (1)$$

where

$$x_1 = y_1 + x \cos\theta + y \sin\theta \quad (2)$$

and

$$\sigma_x = \sigma_y = \sigma \quad (3)$$

We have

$$G(x,y) = exp - \left(\frac{2x_1^2}{\sigma^2}\right) \cos\left(\frac{2\pi x_1}{\lambda}\right) \quad (4)$$

A window size of $15 \times 15$ was used, which proved to give a precise result with less computation load. Since the images contain vessels of varying width, we have used 2 values of $\sigma$, a smaller value for small vessels and a larger value for the large vessels. The thresholding method used in Zhang et al. (2009) has been followed since it can be adapted to the Gabor filter.

(a) Double-sided thresholding

Let '$r(x)$' denote the peak of the truncated Gabor function. The threshold value '$T$' is defined at the points $x = (x + d)$ and $(x - d)$ as in the following inequalities:

$$R(x) - r(x - d) > T \quad (5)$$
$$R(x) - r(x + d) > T \quad (6)$$

Now, '$d$' is obtained by multiplying '$\sigma$' by a constant '$c_d$'

$$T = c_t \times t \quad (7)$$

where $c_t$ is a constant obtained empirically

$$t = r(x) - r(x + d) = r(x) - r(x - d) \quad (8)$$

$$t = 1 - \left(exp^{-\frac{d^2}{2\sigma}}\right) \cos\left(\frac{2\pi d}{\lambda}\right) \quad (9)$$

Note that for the extraction of the smaller vessels the threshold value '$T$' is multiplied by 0.5 (empirical).

Since each convolution result (from each direction) yields in maximum intensity pixels representing vessels in that direction, we compare the pixel values for all the images and choose the maximum intensity value to form the vessel map representing the vessels in all the chosen orientations. We thus have two images for the small vessels and one for the large vessel. In order to deal with the noise in the image, we use the hysteresis thresholding algorithm proposed in Reza (2004).

(b) Hysteresis thresholding

By following this algorithm, first proposed by Canny (1986), we have been able to construct two vessel maps, namely $V_S$ and $V_l$ representing the small vessels and large vessels, respectively. To reconstruct $V_l$, we followed the method used in Zhang et al. (2009), that is, using a lower threshold $T_1$ which is a scaled down version of the higher threshold $T_h$. For obtaining the vessel map representing the small vessels ($V_s$), we have used the images $V_{sh}$, which has been obtained after pre-processing the green channel image with a high clip limit and $V_{sl}$, which has been obtained after the use of a higher clip limit to emphasize the smaller vessels. The image $V_{sl}$ contains the smallest vessels and some noise, whereas $V_{sh}$ has been thresholded to obtain the main small vessels, with the least possible amount of noise. Candidate pixels from $V_{sl}$ are therefore scanned within their neighborhood and tested if they link to vessels in $V_{sh}$. The vessel map $V_s$ is therefore reconstructed. After obtaining the vessel maps, we fuse them by choosing the higher pixel value from each vessel map and putting in the final image $V_f$.

### 2.3. Performance evaluation

For testing our results, we have used the DRIVE database ground truth images and mask images to compare with our results. The sensitivity, specificity and accuracy were found out by com-

**Table 2**
Comparative analysis for vessel extraction.

| With CLAHE | | | | | | | | Without CLAHE | | |
|---|---|---|---|---|---|---|---|---|---|---|
| Image | $T_s$ | $T_l$ | $\beta_s$ | Sensitivity | Specificity | Maximum accuracy | Average accuracy | Sensitivity | Specificity | Maximum accuracy |
| 1 | 0.23 | 0.045 | 0.28 | 0.7002 | 0.9743 | 93.838 | 93.7904 | 0.7008 | 0.9707 | 93.5354 |
| 2 | 0.23 | 0.048 | 0.23 | 0.7159 | 0.9763 | 93.7286 | 93.5918 | 0.6992 | 0.9748 | 93.3537 |
| 3 | 0.23 | 0.025 | 0.25 | 0.6181 | 0.9783 | 92.5822 | 90.6028 | 0.6096 | 0.9737 | 92.0661 |
| 4 | 0.28 | 0.046 | 0.25 | 0.6219 | 0.9796 | 93.1944 | 93.1948 | 0.6435 | 0.9738 | 92.9764 |
| 5 | 0.2 | 0.035 | 0.35 | 0.646 | 0.976 | 93.1241 | 92.8812 | 0.5662 | 0.9814 | 92.5009 |
| 6 | 0.22 | 0.03 | 0.3 | 0.6149 | 0.976 | 92.5055 | 91.8026 | 0.5271 | 0.9828 | 91.8474 |
| 7 | 0.2 | 0.048 | 0.3 | 0.5913 | 0.9783 | 92.7023 | 92.6074 | 0.6224 | 0.9625 | 91.7444 |
| 8 | 0.3 | 0.037 | 0.3 | 0.6056 | 0.9786 | 93.1751 | 93.0499 | 0.5008 | 0.9834 | 92.2765 |
| 9 | 0.2 | 0.036 | 0.3 | 0.6267 | 0.9755 | 93.4525 | 93.239 | 0.5103 | 0.9837 | 92.8125 |
| 10 | 0.25 | 0.038 | 0.3 | 0.6251 | 0.9795 | 93.7154 | 93.667 | 0.5988 | 0.9783 | 93.301 |
| 11 | 0.25 | 0.06 | 0.3 | 0.6024 | 0.9726 | 92.4588 | 91.7112 | 0.5717 | 0.9715 | 91.968 |
| 12 | 0.25 | 0.04 | 0.3 | 0.6385 | 0.9725 | 93.0687 | 93.0327 | 0.6442 | 0.9701 | 92.9312 |
| 13 | 0.2 | 0.042 | 0.3 | 0.6461 | 0.973 | 92.6615 | 92.6541 | 0.6217 | 0.9705 | 92.1055 |
| 14 | 0.26 | 0.05 | 0.22 | 0.6341 | 0.9816 | 94.0621 | 93.8912 | 0.6325 | 0.9778 | 93.707 |
| 15 | 0.24 | 0.06 | 0.22 | 0.6291 | 0.9798 | 94.3393 | 93.4853 | 0.6204 | 0.9769 | 93.9902 |
| 16 | 0.2 | 0.046 | 0.3 | 0.6447 | 0.976 | 93.2695 | 93.2348 | 0.6747 | 0.9707 | 93.1983 |
| 17 | 0.2 | 0.035 | 0.35 | 0.6439 | 0.9772 | 93.6144 | 93.4369 | 0.6407 | 0.9777 | 93.6118 |
| 18 | 0.2 | 0.052 | 0.15 | 0.6358 | 0.9764 | 93.7284 | 93.6106 | 0.6872 | 0.9685 | 93.6168 |
| 19 | 0.2 | 0.037 | 0.35 | 0.7371 | 0.9779 | 94.8885 | 94.746 | 0.6934 | 0.9753 | 94.1338 |
| 20 | 0.2 | 0.045 | 0.25 | 0.65 | 0.9746 | 94.0006 | 93.9676 | 0.6874 | 0.9711 | 94.0889 |
| Average values | 0.227 | 0.0427 | 0.28 | 0.6413 | 0.9767 | 93.4054 | 93.1098 | 0.62263 | 0.9747 | 92.9882 |

paring the results with the ground truth images. Maximum average accuracy (MAA) over the 20 test images of the DRIVE database was computed and average of those parameters was used to generate the average accuracy for each image. Considering the pixels in the field of view (FOV),

$$Sensitivity = \frac{\sum Correctly\ classified\ vessel\ pixels}{\sum No.\ of\ vessel\ pixels\ in\ ground\ truth} \quad (10)$$

$$Specificity = \frac{\sum Correctly\ classified\ background\ pixels}{\sum No.\ of\ background\ pixels\ in\ ground\ truth} \quad (11)$$

$$Accuracy = \frac{\sum Correctly\ classified\ pixels\ (vessel\ and\ background)}{Total\ no.\ of\ pixels\ in\ ground\ truth} \quad (12)$$

## 3. Results and discussion

The experiment was performed for the set of 20 test images of the DRIVE database on a 1.66 GHz processor. The time taken for the segmentation process of each image was approximately 20 s. Using the above testing algorithm, we found out the maximum average accuracy (MAA) for each image by varying the threshold parameters for large and small vessels, $T_s$ and $T_l$, respectively, and the clip limit $\beta_s$ for the small vessels. The clip limit for the larger vessels was kept constant at 0.01. An average of the optimal parameters was computed for the 20 images and by setting $T_s$, $T_l$ and $\beta_s$ to their corresponding average optimal values, the average accuracy was calculated (see Tables 1 and 2).

The proposed technique for vessel segmentation provides better average accuracy (93.1%) as well as maximum average accuracy (93.4%) as compared to the maximum average accuracy (92.9%) obtained without CLAHE.

## 4. Conclusion

The main contribution of this technique is in the detection of small vessels using an appropriate preprocessing technique, which proves to be useful in enhancing the contrast without causing an increase in the number of false positives. Compared to other vessel extraction techniques which do not require a supervised method, this technique provides a very high accuracy and sensitivity. Moreover, the accuracy can further be increased by making use of higher resolution images than that of the DRIVE database. Furthermore,

the algorithm can be tuned (by changing the vessel widths and threshold values) so as to obtain the desired result, depending on the pathology. This gives us an edge over other supervised techniques towards the diagnosis of PDR wherein neovascularization detection is of great importance. The main drawback of this approach is that for each set of images, the threshold has to be manually set to for the best result.

## References

Alex Stark, J. (2000). Adaptive image contrast enhancement using generalizations of histogram equalization. *IEEE Transactions on Image Processing, 9*(5).

Al-Rawi, M., Qutaishat, M., & Arrar, M. (2009). An improved matched filter for blood vessel detection of digital retinal images. *Computers in Biology and Medicine, 37*, 262–267.

Canny, J. (1986). A computational approach to edge detection. *IEEE Transactions on Pattern Analysis and Machine Intelligence, PAMI-8*(6).

Chaudhuri, S., Chatterjee, S., Katz, N., Nelson, M., Goldbaum, M., et al. (1989). *IEEE Transactions in Medical Imaging, 8*(3), 263–269.

Niemeijer, M., Staal, J., Van Ginneken, B., Loog, M., & Abràmoff, M. D. (2009). Comparative study of retinal vessel segmentation methods on a new publicly available database. *Lecture Notes in Computer Science. Computer Analysis of Images and Patterns* (Vol. 5702). Berlin/Heidelberg: Springer.

Odstrčilík, J., Jan, J., Gazárek, J., & Kolář, R. (2009). Improvement of vessel segmentation by matched filtering in colour retinal images. *IFBME Proceedings* (Vol. 25/11, pp. 327–330). Berlin, Heidelberg: Heidelberg.

Pang, K. Y., Iznita, L. I., Ahmad Fadzil, M. H., Hanung, A. N., Hermawan, N., & Vijanth, S. A. (2009). *Segmentation of retinal vasculature in colour fundus images*. In *Conference on innovative technologies in intelligent systems and industrial applications (CITISIA 2009), Monash University, Sunway campus, Malaysia*.

Reza, A. M. (2004). Realization of the contrast limited adaptive histogram equalization (CLAHE) for real-time image enhancement. *Journal of VLSI Signal Processing, 38*, 35–44.

World Health Organization Media Centre, Fact sheet No. 312 (November 2009). <http://www.who.int/mediacentre/factsheets/fs312/en/last> Accessed April 2010.

Zhang, M., Wu, D., & Liu, J. (2005). On the small vessel detection in high resolution retinal images. In *Proceedings of the 2005 IEEE transactions in medicine and biology 27th annual conference, Shangai, China*.

Zhang, L., Li, Q., You, J., & Zhang, D. (2009). A modified matched filter with double-sided thresholding for screening proliferative diabetic retinopathy. *IEEE Transactions on Information Technology in Biomedicine, 13*(4).